

# The Magnetic Phase Transition and Excitations in the Frustrated Antiferromagnet $\text{ZnCr}_2\text{O}_4$

An Experiment Using the SPINS Triple-Axis Spectrometer

Summer School on Methods and Applications of Neutron Spectroscopy

NIST Center for Neutron Research

June 18-22, 2001

Seung-Hun Lee, Peter Gehring, and Young Lee

## OBJECTIVES

1. To understand what is measured in a neutron inelastic scattering experiment.
2. To gain a basic understanding of the principles of Triple-Axis Spectroscopy (TAS).
3. To gain experience with the use of a Position Sensitive Detector (PSD) to obtain neutron elastic and inelastic scattering data.
4. To learn how to analyze the TAS data obtained to extract physical information about the system being studied.
5. To study the magnetic phase transition and associated dynamics in the geometrically frustrated antiferromagnet  $\text{ZnCr}_2\text{O}_4$ .

## I. INTRODUCTION

It is the ability of the neutron to exchange a *measurable* amount of energy with a liquid or solid sample that makes it useful as a probe of the various dynamical phenomena in condensed matter systems. Typical neutron energies available at a reactor source can range from 100 – 500 meV (hot), to 5 – 100 meV (thermal), to 0.1 – 10 meV (cold), where 1 meV =  $10^{-3}$  eV =  $8.06 \text{ cm}^{-1}$ . A number of different methods can be used to prepare a monochromatic (or monoenergetic) neutron beam having energies that are comparable in magnitude to, for example, those of the lattice vibrations in a solid (phonons), the spin excitations in a magnetic system (magnons), the torsional, bending, or stretching vibrations of a polymer chain, or the rotational motions in a molecular solid (librons). As a result it is usually quite easy to detect the change in the neutron energy after scattering from a sample since the energy transferred to or from the sample  $\Delta E = E_i - E_f$  generally represents a significant fraction of the initial and final neutron energies  $E_i$  and  $E_f$ .

The energy  $\Delta E$  transferred during the interaction between neutron and sample can be used to create an excitation (such as a phonon or magnon) of the system, in which case the neutron loses an amount of energy  $\Delta E$  equal to the energy of the excitation. Conversely, the same excitation can give up its energy to the neutron, in which case the excitation is said to be annihilated. In either case, the physics of the excitation as revealed by the absolute change in the neutron energy is the same. The energy transfer  $\Delta E$  is often expressed as a frequency of vibration through the relation

$$\Delta E = \hbar\omega, \tag{1}$$

where  $2\pi\hbar = h = 6.626 \times 10^{-34}$  Joules-seconds is Planck's constant, and  $\omega$  is the frequency of vibration of the excitation. Since frequency and time are inversely related, the neutron energy transfer  $\hbar\omega$  reflects the *time scale* of the dynamics.

**Question:** Estimate the value of  $(\Delta E/E_i)$  required to observe an optic phonon with an energy of 10 meV using x-ray, light, and neutron scattering techniques assuming the respective values of 7,000 eV, 2 eV, and 30 meV (0.030 eV) for  $E_i$ . Which technique is best suited for this measurement?

In addition to having energies that are well adapted to the study of a large variety of dynamical phenomenon, neutrons also possess the ability to provide, simultaneously, unique information about the *geometry* of these dynamics through the exchange of momentum with the sample. This is done by measuring in what directions (i. e., through what angles) the neutrons scatter. The momentum of a neutron varies inversely with the neutron wavelength  $\lambda$ , and hence an accurate measure of the momentum transferred between sample and neutron during the scattering process will in turn provide information about the spatial scale of the dynamics being probed. Such an accurate measure is relatively easy to obtain as long as the neutron wavelength is comparable to the length scale of the motions of interest.

**Question:** The relationship between wavelength and energy for the neutron is given by:

$$E = \frac{h^2}{2m\lambda^2} = 81.81(\text{meV} \cdot \text{\AA}^2)/\lambda^2, \quad (2)$$

where  $m = 1.675 \times 10^{-24}$  grams is the mass of the neutron. Using this equation, estimate the wavelengths corresponding to hot, thermal, and cold neutrons available at a reactor source. How do these wavelengths compare with the length scales associated with the dynamics or motions you are specifically interested in?

In the following sections we will discuss the partial differential scattering cross section, which is the actual physical quantity that is measured by neutron spectroscopy. We then outline the basic operating principles behind a triple-axis spectrometer (TAS), the concept

for which Bertram Brockhouse earned the 1994 Nobel prize in physics shared jointly with Clifford Shull.

### A. The Partial Differential Scattering Cross Section $\frac{d^2\sigma}{d\Omega dE_f}$

Most neutron spectroscopic techniques can be reduced to a measurement of what is called the *partial differential scattering cross section*, or  $d^2\sigma/d\Omega dE_f$ , as a function of the neutron energy transfer  $\hbar\omega$  and the neutron momentum transfer  $\vec{Q}$ . The quantity  $\vec{Q}$  is known as the scattering vector, and has units of inverse length. In the scattering process between the neutron and the sample, the total momentum and energy of the system are conserved, i. e.

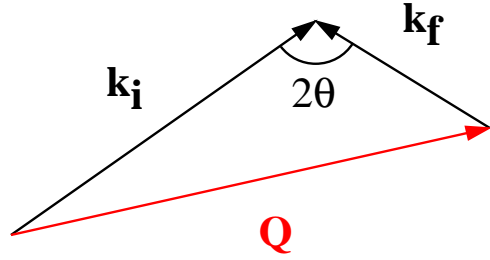
$$\vec{Q} = \vec{k}_i - \vec{k}_f, \quad (3)$$

$$\hbar\omega = E_i - E_f = \Delta E. \quad (4)$$

Hence the energy or momentum lost (or gained) by the neutron when it scatters from a sample is gained (or lost) by the sample. In the previous equation, the quantities  $\vec{k}_i$  and  $\vec{k}_f$  refer to the initial and final neutron wavevector, respectively, and point in the direction of the incident and final (scattered) neutron beam. The relationship between  $\vec{k}_i$ ,  $\vec{k}_f$ , and  $\vec{Q}$  can be represented by the *scattering triangle* shown in Fig. 1. The magnitude of the neutron wavevector  $k$  is  $2\pi/\lambda$ , and is related to the neutron energy via

$$E = \frac{(\hbar k)^2}{2m} = 2.072(\text{meV} \cdot \text{\AA})k^2, \quad (5)$$

From this last equation, one can obtain the second equation in Fig. 1 which relates the energy transfer to the magnitude of the initial and final wavevectors. The angle between  $\vec{k}_i$  and  $\vec{k}_f$  is commonly denoted by  $2\theta$ , and thus represents the total angle through which a neutron is scattered by the sample. Note that the convention followed in this summer school is such that the energy transfer  $\hbar\omega$  is positive when  $E_i > E_f$ , i. e. when the neutron loses energy to the sample during the scattering process. This convention of defining when  $\hbar\omega$  is positive varies among neutron scattering facilities.



$$\mathbf{Q} = \mathbf{k}_i - \mathbf{k}_f$$

$$\hbar\omega = \frac{\hbar^2}{2m} (k_i^2 - k_f^2)$$

Fig. 1. Scattering triangle. The neutron is scattered through the angle  $2\theta$  and the scattering vector,  $\vec{Q}$ , is given by the vector relationship  $\vec{Q} = \vec{k}_i - \vec{k}_f$ .

The partial differential scattering cross section is defined as the total number of neutrons scattered per second by the sample into a unit of solid angle  $d\Omega$  in a given direction, having final energies  $E$  that lie between  $E_f$  and  $E_f + dE_f$ . It is normalized by the neutron flux incident on the sample  $\Phi_0$  (measured in neutrons/sec/cm<sup>2</sup>) so that it has units of area/(solid angle)/energy. If one integrates the partial differential scattering cross section over all solid angle ( $4\pi$  steradians), and all final energies ( $0 \leq E_f \leq \infty$ ), one obtains the total number of neutrons scattered out of the beam per second by the sample. (This assumes that the absorption of neutrons by the sample, which can often occur, is negligible.) This is known as the total scattering cross section  $\sigma$ , which has units of area. Thus  $\sigma$  represents the scattering strength of the sample, and can be viewed as an unnormalized probability that an incident neutron will be scattered. If one compares the value of  $\sigma$  for hydrogen with that of aluminum, it will be clear that different elements can have enormously different scattering strengths.

**Question:** The scattering cross section for x-rays is a severe and monotonically increasing function of atomic number  $Z$ . This is because x-rays scatter from the electrons of an atom, which increases with increasing  $Z$ . Neutrons, by contrast, scatter from the atomic nucleus via short-range nuclear forces. If you plot  $\sigma$  for neutrons versus  $Z$ , do you see any trend? In what ways might this be advantageous? (Values for  $\sigma$  can be obtained from the NCNR Summer School webpage under “Course Materials.”)

It is instructive to consider the relative sizes of  $\sigma$  and  $d^2\sigma/d\Omega dE_f$ . Clearly  $\sigma$ , which represents the total number of neutrons scattered per second by the sample, is many orders of magnitude larger than  $d^2\sigma/d\Omega dE_f$ , which is both an energy and directionally analyzed quantity. On the other hand, the partial differential scattering cross section provides a correspondingly greater amount of information because it contains all of the details of the individual and collective motions of the atoms, molecules, and/or any atomic magnetic moments that comprise the sample. The *differential cross section*  $d\sigma/d\Omega$ , which is what is measured in a diffraction experiment, lies between  $\sigma$  and  $d^2\sigma/d\Omega dE_f$  in size. As the elastic component dominates in  $d\sigma/d\Omega$ , it gives the time-averaged (equilibrium) positions of all of the nuclei in the sample, and is used to determine the crystal structure.

The partial differential scattering cross section can be cast into a useful mathematical form via the formalism outlined at the end of the neutron scattering primer written by Roger Pynn (which the summer student is presumed to have read). With a small deviation from the notation used by Pynn we can write the partial differential cross section for a system composed of a single atomic element as

$$\frac{d^2\sigma}{d\Omega dE_f} = \frac{1}{4\pi} \left( \frac{k_f}{k_i} \right) \left[ \sigma_{coh} S_{coh}(\vec{Q}, \omega) + \sigma_{inc} S_{inc}(\vec{Q}, \omega) \right], \quad (6)$$

where  $S(\vec{Q}, \omega)$  is exactly same quantity as  $I(\vec{Q}, \epsilon)$  used by Pynn to express Van Hove’s “scattering law.” The subscripts “coh” and “inc” refer to the coherent and incoherent parts of the scattering, and pertain to the collective or individual motions of the atoms,

respectively, as described on page 9 of Pynn’s primer. For the purposes of this experiment on SPINS, we are only concerned with the collective dynamics of the magnetic moments present in  $\text{ZnCr}_2\text{O}_4$ , and thus the coherent part of the partial differential scattering cross section.

The scattering function  $S_{coh}(\vec{Q}, \omega)$  contains a double sum over pairs of nuclei as shown in Eq. 3 on page 28 of Pynn’s primer. Each term in this sum represents the “correlation” between the position of one nucleus at a time  $t = 0$  with that of another nucleus at an arbitrary time  $t$  later. These correlations are important for systems in which the nuclei are strongly coupled via some type of interaction, and less so when this coupling is weak. In either case  $S_{coh}(\vec{Q}, \omega)$  provides a measure of the strength of this coupling, and hence the resulting “collective” motions. It is therefore extremely useful, for example, in mapping out the dispersion relations of lattice vibrations, that is how the energy  $\omega$  of the lattice vibrations changes at different  $\vec{Q}$  positions, in solids. For the remainder of this discussion, we will drop the subscript “coh” with the understanding that we are referring to the coherent part of the scattering function.

The scattering function  $S(\vec{Q}, \omega)$  can be simply related to the imaginary part of the dynamical susceptibility according to

$$S(\vec{Q}, \omega) = \frac{\hbar}{\pi} \left( \frac{1}{\frac{\hbar\omega}{k_B T} - 1} + 1 \right) \chi''(\vec{Q}, \omega), \quad (7)$$

where  $k_B = 1.381 \times 10^{-23}$  Joules/K is Boltzmann’s constant (note:  $\hbar/k_B = 11.60$  K/meV is a handy conversion factor). This is a very important equation since it shows that  $S(\vec{Q}, \omega)$ , which is readily obtained from the experimentally measured partial differential scattering cross section via Eq. 6, is also related to a quantity that is easily calculated by theorists,  $\chi''(\vec{Q}, \omega)$ . Therefore a measurement of the partial differential scattering cross section via neutron spectroscopy allows for a direct test of theoretical models. By recording the scattered neutron intensity as a function of energy transfer  $\hbar\omega$  and momentum transfer  $\vec{Q}$ , and removing the instrumental effects, one obtains  $S(\vec{Q}, \omega)$ , which contains all of the dynamical information about the system.

With the exception of the neutron spin-echo (NSE) technique, all other neutron spectroscopic methods measure  $d^2\sigma/d\Omega dE_f$  using a neutron detector to count the number of neutrons scattered per unit time from a sample as a function of the energy transfer  $\Delta E = \hbar\omega$  and the momentum transfer  $\vec{Q}$ . To do this requires that one know the energy and wavevector of the neutron before  $(E_i, \vec{k}_i)$  and after  $(E_f, \vec{k}_f)$  it scatters from the sample. There are many ways of doing this, and most will be illustrated by the different experiments in this summer school. As will be seen, each method has its own particular advantages and limitations, depending on the range of energy transfers (time scales) and momentum transfers (length scales) one wishes to study.

## B. The Triple-Axis Spectrometer

The triple-axis spectrometer (TAS) is an extremely versatile instrument that is primarily intended for the study of the collective motions of the atoms and their magnetic moments in single crystal samples. The first TAS system was used to obtain the first experimental demonstration of phonon and magnon dispersion curves (in aluminum and magnetite) in the mid 1950's. The instrument derives its name from the fact that the neutrons interact with three crystals on their way from reactor to detector, each crystal being able to rotate independently about a vertical axis passing through its center. This is shown schematically in Fig. 2. The first crystal is called the monochromator, as it selects a single monochromatic component from the white neutron beam emanating from the reactor. The second crystal is the sample itself (although it may be either a single crystal or a powder). The third crystal is called the analyzer, as it is used to analyze the energy spectrum of the neutron beam that scatters from the sample. And the last primary element of the instrument is, of course, the neutron detector.

In a triple-axis spectrometer, the initial and final neutron energies are determined by exploiting the process of Bragg diffraction from the monochromator and analyzer single crystals. This is done by rotating the crystals about their respective vertical axes such that



a specific set of atomic Bragg planes, having a well-defined interplanar spacing  $d$ , makes an angle  $\theta$ , known as the Bragg angle, with respect to the initial (or scattered) beam direction. When this is done, only neutrons with wavelengths that satisfy the Bragg condition (see pages 9-11 of Pynn's primer)

$$n\lambda = 2d \sin \theta, \tag{8}$$

where  $n$  is an integer greater than zero, will Bragg scatter from each crystal and proceed successfully to the next element of the spectrometer.

**Question:** Because the variable  $n$  in Bragg's law can be any integer greater than zero, more than one monochromatic component can be present in the neutron beam diffracted by either monochromator or analyzer. List the possible wavelengths of these other components. How might their presence affect the experimental data?

To remove the extra and unwanted monochromatic components from a Bragg diffracted beam, while preserving the neutron flux at the desired fundamental ( $n=1$ ) wavelength  $\lambda$ , it is common practice to place a filter composed of some solid material in the path of the beam. The choice of material depends on the primary wavelength  $\lambda$ . For thermal neutrons, a special form of graphite (pure carbon) known as highly-oriented pyrolytic graphite (HOPG or just PG) is often used. Graphite has a layered structure in which the crystalline [001] or  $c$ -axis is normal to the layers. HOPG behaves like a crystal of graphite in which the various graphite layers have all been randomly spun about the  $c$ -axis. Therefore HOPG can be viewed as a single-crystal along [001], and a powder along the two orthogonal directions. It exhibits very good transmission at certain neutron energies including 13.7, 14.7, 30.5, and 41 meV. Neutrons of other energies are preferentially (though not completely) scattered out of the beam, thereby minimizing the chance they will enter the detector and contribute to the background.

For cold neutrons, such as those used on the SPINS spectrometer, a polycrystalline block of beryllium (Be) is used as a wavelength filter. The requirement for this filter to work is that there be enough tiny crystallites to span all angular orientations, i. e. all values of the Bragg angle  $\theta$ , so that all unwanted neutrons are Bragg scattered out of the neutron beam.

**Question:** Consider a white (polychromatic) beam incident on a polycrystalline Be filter. What happens to those neutrons with wavelengths  $\lambda > 2d_{max}$ , where  $d_{max} = 1.98 \text{ \AA}$  is the largest interplanar  $d$  spacing available in beryllium? What happens to those neutrons with  $\lambda \leq 2d_{max}$ ? Make a simple sketch of transmission versus energy for this filter.

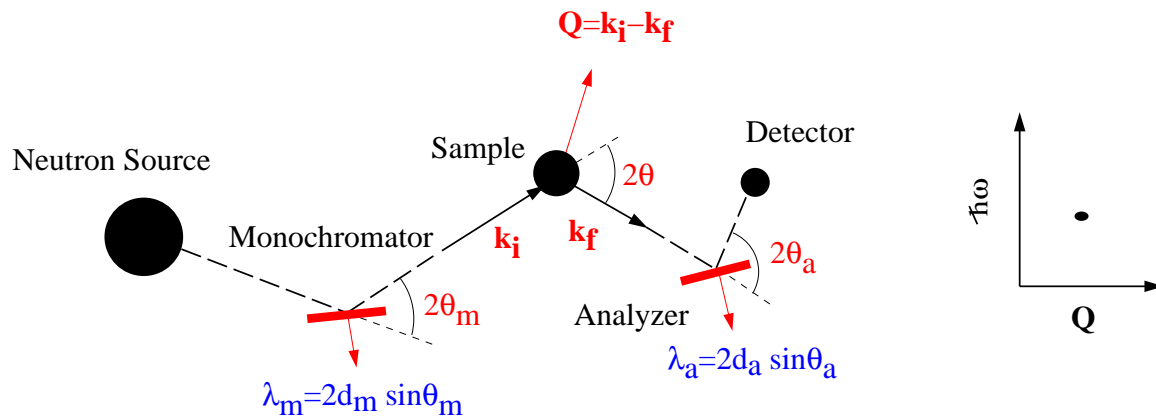


Fig. 2. Schematic scattering configuration for a conventional triple-axis spectrometer. It measures a scattering event at a single value of  $(\vec{Q}, \hbar\omega)$  at a time.

As can be seen from Fig. 2, when the incident neutron beam from the reactor strikes the monochromator, it is scattered through an angle  $2\theta_m$  from its initial direction. This is commonly referred to as the monochromator *scattering angle*. In order for the resulting monochromatic beam to hit the sample, it is necessary to rotate the subsequent elements (sample, analyzer, and detector) of the spectrometer about the monochromator axis through an angle of  $2\theta_m$ . The same situation applies for the sample, and the analyzer, i. e. associated with each crystal is a Bragg angle  $\theta$ , and a scattering angle  $2\theta$ . Hence each axis of the triple-

axis spectrometer is actually composed of two motors, one to control the crystal Bragg angle  $\theta$ , and the other to rotate the subsequent (downstream) elements of the instrument by the appropriate scattering angle  $2\theta$ . While there are many different motors involved in the operation of a triple-axis spectrometer, such as those that control mechanical slits that limit the horizontal and vertical extent of the neutron beam, the primary instrument motors are those that control the values of  $\theta$  and  $2\theta$  for the monochromator, sample, and analyzer.

The material most commonly used as monochromator and analyzer in a TAS system is also HOPG. Its utility lies in its very high reflectivity for neutrons over a wide range of energy. The (002) Bragg planes of HOPG have an interplanar  $d$  spacing of 3.354 Å. Other materials that also find use in triple-axis spectroscopy are silicon, germanium, and copper.

**Question:** Calculate the monochromator Bragg and scattering angles required to obtain a neutron beam having initial energies  $E_i = 14.7$  meV, and 100 meV using the (002) reflection of HOPG. The (220) reflection of copper has a  $d$  spacing of 1.278 Å. Would this be a better choice of monochromator in either case?

During the interaction with the sample, neutrons can lose or gain energy, and thus can emerge with an energy  $E_f \neq E_i$ . The resulting energy transfer can be computed according to

$$\hbar\omega = E_i - E_f = \frac{h^2}{8m} \left( \frac{1}{d_m^2 \sin^2 \theta_m} - \frac{1}{d_a^2 \sin^2 \theta_a} \right), \quad (9)$$

where  $d_m$  and  $d_a$  are the  $d$ -spacings of the monochromating and analyzing crystals, respectively. If the analyzer is set to select the same energy as that of the incident beam ( $E_i = E_f$ ), then  $\hbar\omega = 0$ , and the scattering is said to be *elastic*. If not, one detects *inelastic* scattering events. (A third category of scattering known as *quasielastic* scattering, is discussed in the experiment on the Disc Chopper Spectrometer (DCS).)

Controlling the momentum transfer  $\vec{Q}$  between neutron and sample is achieved by orienting the incident and final neutron wavevectors with respect to each other to obtain the

desired vector difference ( $\vec{k}_i - \vec{k}_f$ ). Unlike the case of the monochromator and analyzer crystals, the Bragg and scattering angles for the sample needn't be related by a simple factor of 2. Indeed, when measuring inelastic scattering they usually are not. Hence the notation  $2\theta$  (which is quite common) can be misleading for the novice scatterer. With this warning in mind, we can calculate the magnitude of the momentum transfer by computing the vector dot product of  $\vec{Q}$  with itself, i. e.

$$\vec{Q} \cdot \vec{Q} = (\vec{k}_i - \vec{k}_f) \cdot (\vec{k}_i - \vec{k}_f), \quad (10)$$

from which we obtain

$$Q = \sqrt{k_i^2 + k_f^2 - 2k_i k_f \cos 2\theta}. \quad (11)$$

Note that the momentum transfer does not depend on the sample Bragg angle  $\theta$ , but only on the sample scattering angle. The purpose of the Bragg angle is to allow the crystalline axes of the sample (if it happens to be a single crystal) to be aligned in specific ways with respect to the scattering vector  $\vec{Q}$ . This allows one to probe the geometry of the dynamics in question along different symmetry directions. The utility of the sample Bragg angle becomes moot, however, in the case of a powder sample (composed of many tiny and randomly-oriented single crystals).

**Question:** What is the maximum momentum transfer one can obtain in the case of elastic scattering, i.e.  $|\vec{k}_i| = |\vec{k}_f|$ ? What is the minimum? Why might these two configurations be problematic from an experimental point of view?

By stepping the analyzer Bragg angle  $\theta_a$ , or the monochromator Bragg angle  $\theta_m$ , by computer in small angular increments, one can effectively scan the energy transfer  $\hbar\omega$ . Generally this is done while keeping the momentum transfer  $\vec{Q}$  constant, and is known as a constant- $\vec{Q}$  scan. The complement to the constant- $\vec{Q}$  scan is the constant- $E$  scan in which the energy transfer is held constant while one varies the momentum transfer. These two

scans are fundamental to the triple-axis method, and are used commonly to map out the dispersion relations for both phonons and magnons in condensed matter systems.

In the case of the constant- $\vec{Q}$  scan one has a choice of which Bragg angle to vary, and which to hold fixed. As a rule, it is best not to vary both as one needs to place a wavelength filter in the path of either the incident beam (before the sample) or the scattered beam (after the sample) in order to remove the higher order harmonic content of the Bragg diffracted neutron beam (remember the effect of the integer  $n$  in Bragg's law). If the analyzer angle  $\theta_a$  is fixed and one varies  $\theta_m$ , the result is an  $E_f$ -fixed configuration. Doing the opposite results in an  $E_i$ -fixed configuration. Both methods yield data that contain the same physics. Deciding which to choose depends largely on the specific problem being studied.

Because of the small size of the partial differential scattering cross section, and the limited flux available at neutron sources, neutron spectroscopic methods cannot make measurements at arbitrarily precise values of  $\hbar\omega$  and  $\vec{Q}$ . To boost the neutron signal at the detector, the experimentalist is obliged to work with beams of neutrons having wavevectors that are not exactly parallel, i. e. which have finite vertical and horizontal angular divergences. This introduces a spread or uncertainty to the momentum transfers of the neutrons which are centered about some average value  $\vec{Q}_0$ . The beam divergences are controlled by introducing sets of thin parallel blades called collimators into the beam whose length  $L$  and separation  $v$  define the limiting divergence  $\eta$  of the neutrons according to

$$\eta = 2 \tan^{-1}(v/L) \approx 2v/L. \quad (12)$$

These blades are coated with a strongly neutron absorbing material such as  $\text{Gd}_2\text{O}_3$  or Cd such that neutrons with a divergence that exceeds  $\eta$  are absorbed and removed from the beam. Typically collimators are inserted in each of the four different flight paths between elements of the spectrometer, i.e. between reactor and monochromator, monochromator and sample, etc. A choice of fine collimation improves the instrumental  $\vec{Q}$ -resolution at the expense of neutrons counted at the detector. A choice of coarse resolution degrades the  $\vec{Q}$ -resolution, but increases the neutron count rate. To optimize the experimental data then,

it is best to match the  $\vec{Q}$ -resolution of the instrument with the features of the scattering one is try to measure.

Similarly, one can coarsen the instrumental  $\hbar\omega$ -resolution by introducing small angular misorientations of the Bragg planes into the monochromator and analyzer crystals. This can be done by pressing the crystals under high pressure and temperature, such that the Bragg planes are no longer exactly parallel to each other, but are instead narrowly distributed in angle about some average. Such an angular distribution is often Gaussian in form, and is usually characterized by the half-width at half maximum (HWHM), known as the crystal mosaic. The result is that both monochromator and analyzer will diffract a narrow spread of neutron energies that depends on the size of the mosaic, and significantly increases the scattering intensity measured at the detector. Typical values for the mosaic spread range from 30' (0.5°) to 40'. The resulting energy transfers of the neutrons will be distributed about an average value  $\hbar\omega_0$ .

In general, the instrumental  $(\vec{Q}, \hbar\omega)$ -resolution is a complicated function of  $\vec{k}_i$ ,  $\vec{k}_f$ , collimator divergences, and the monochromator and analyzer mosaic spreads. For a given spectrometer configuration, the instrumental resolution can be expressed as a four-dimensional function of  $\hbar\omega$  and  $\vec{Q}$  as  $R(\vec{Q} - \vec{Q}_0, \omega - \omega_0)$ , and is always calculated by computer. While one can often extract meaningful results from TAS measurements without needing to take the effects of the finite instrumental resolution into account, all data must be corrected for these effects before they can be compared to theoretical calculations of the scattering function  $S(\vec{Q}, \omega)$ . Fortunately, the intensity at the detector is well-described by a convolution of the resolution function with the scattering function, i. e.

$$I_d(\vec{Q}_0, \omega_0) = \int R(\vec{Q} - \vec{Q}_0, \omega - \omega_0) S(\vec{Q}, \omega) d\vec{Q} d\omega. \quad (13)$$

While a detailed discussion of  $R$  is beyond the scope of this handout, all users of triple-axis spectrometers will need to know how to optimize the instrumental resolution to match the time scales and length scales of the problem they wish to study.

### C. The NCNR Spin Polarized Inelastic Neutron Scattering (SPINS) Spectrometer

The advantage of the triple-axis method is its ability to measure the scattering function  $S(\vec{Q}, \omega)$  at a single value of  $(\vec{Q}, \hbar\omega)$  at a time with a high signal-to-background ratio. By the same token, the disadvantage of the triple-axis method is that it can only measure the scattering function  $S(\vec{Q}, \omega)$  at a single value of  $(\vec{Q}, \hbar\omega)$  at a time so a full set of measurements require extended periods of time. To address this problem, the design of the SPINS instrument incorporates two novel elements to increase its data acquisition rate far beyond that available on a conventional TAS. Both are shown schematically in Fig. 3.

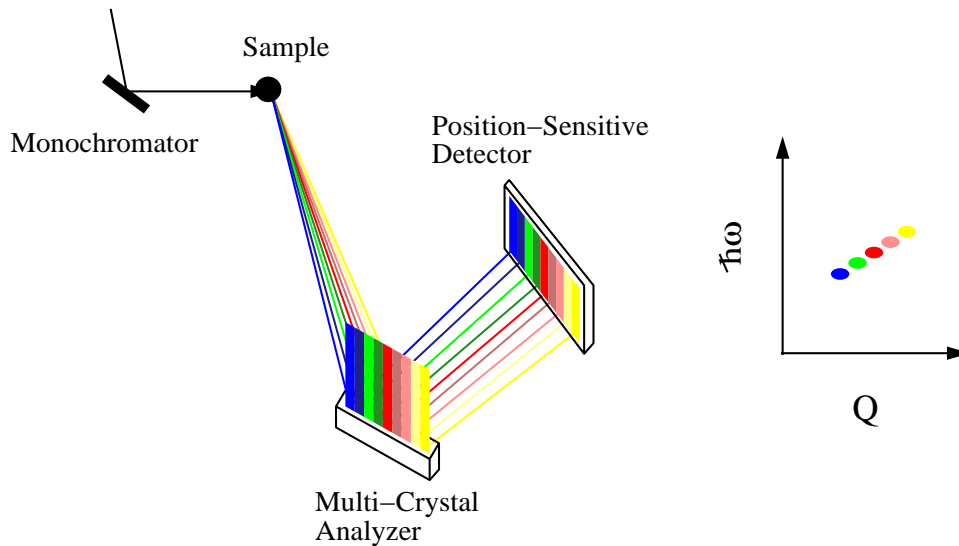


Fig. 3. Schematic scattering configuration of a multiplexing detection system utilizing a Position-Sensitive-Detector (PSD) for a triple-axis spectrometer. It simultaneously measures scattering events at different values of  $(\vec{Q}, \hbar\omega)$  at a time.

First, the lone pencil-shaped neutron detector has been replaced by a two dimensional position sensitive detector (PSD), which covers a much larger angular range of scattering from the sample. Second, the single crystal analyzer concept present in conventional TAS systems has been replaced by a multiple single-crystal analyzer. The SPINS analyzer is composed of 11 narrow blades, each 15 cm tall by 2 cm wide, that are free to rotate about their own vertical axes, whereas the entire analyzer assembly is able to rotate about a central

vertical axis. The combination of the PSD and the multi-crystal analyzer enables SPINS to measure  $S(\vec{Q}, \omega)$  over a range different energy and momentum transfers simultaneously.

When the multiple-crystal analyzer is set to be flat, each blade of the analyzer will diffract neutrons of a different energy  $E_f$  to a different location on the PSD. This is so because each blade makes a slightly different angle  $\theta_j$  with respect to the beam scattered from the sample. For a given incident neutron energy  $E_i$  and sample scattering angle  $2\theta$ , the resulting set of wavevector and energy transfers constitutes a curve in  $(Q, \hbar\omega)$ -space, and is illustrated in the right-hand side of Fig. 3 (compare this to Fig 2). By changing the incident energy and the scattering angle, we can sweep this curve through  $(Q, \hbar\omega)$ -space, thereby surveying the partial differential scattering cross section far more rapidly than a conventional TAS system ever could. A significant advantage of this mode of operation is that the instrumental energy and wavevector resolution, as well as the signal-to-noise ratio, remain as good as they were for the conventional triple-axis spectrometer configuration with the same horizontal collimations. The data acquisition rate, however, is increased by about an order of magnitude.



## II. FRUSTRATED ANTIFERROMAGNETISM IN $\text{ZnCr}_2\text{O}_4$

The system we have chosen to demonstrate the utility of the triple-axis technique is  $\text{ZnCr}_2\text{O}_4$ . This compound is an interesting system because it undergoes a well-defined magnetic phase transition from a paramagnetic state to an antiferromagnetic (AFM) state at  $T=12.5$  K, and, as we will see, the dynamics of the magnetism in these two phases are strikingly different.

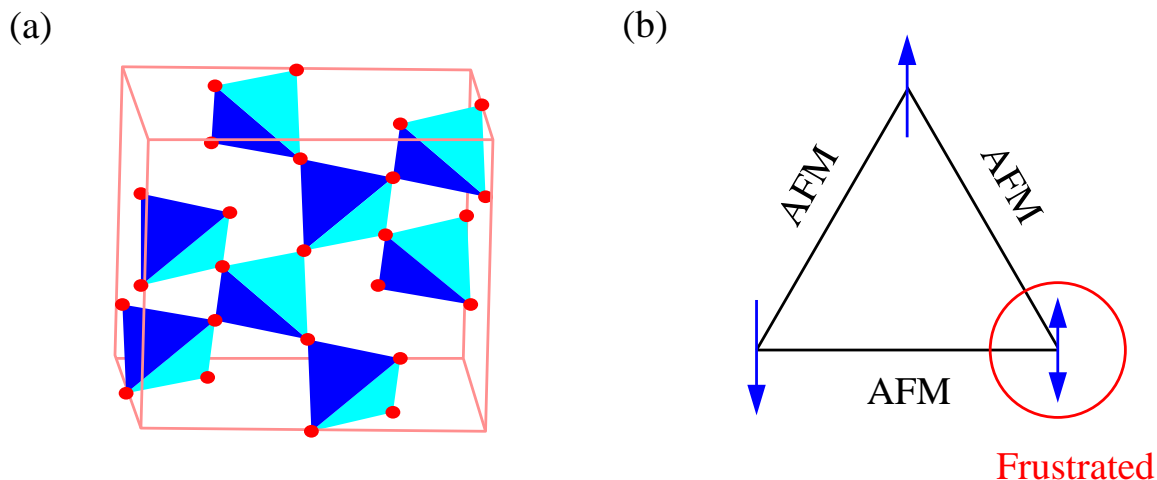


Fig. 4. (a) Sites of  $\text{Cr}^{2+}$  ions in  $\text{ZnCr}_2\text{O}_4$  form a network of corner-sharing tetrahedra. (b) Antiferromagnetic Ising triangles.

The  $\text{Cr}^{3+}$  ions in  $\text{ZnCr}_2\text{O}_4$  possess an electronic spin  $S = 3/2$ , and carry a net magnetic moment of 1.5 Bohr magnetons ( $1.5 \mu_B$ ). These ions form a network of corner-sharing tetrahedra, as shown in Fig. 4 (a). If the magnetic moments in such a network interact *antiferromagnetically* with their nearest neighbors through the Heisenberg exchange Hamiltonian,  $H$ , with a coupling constant  $J$

$$H = -J \sum \vec{S}_i \cdot \vec{S}_j, \quad (14)$$

which the  $\text{Cr}^{3+}$  moments in  $\text{ZnCr}_2\text{O}_4$  do, then the exchange interactions will favor an *antiparallel* alignment of all neighboring moments. However, this condition cannot be satisfied

simultaneously for all neighboring moments because the intrinsic symmetry of the lattice does not allow it. This is an example of *geometrical frustration*. The simplest case of this is a triangle of antiferromagnetically-interacting Ising spins (which can only point up or down) shown in Fig. 4 (b). (Note: the word “spin” is used fairly interchangeably with the term “magnetic moment.”) Here when two spins are aligned antiparallel to each other, as are the top and left hand spins (symbolized by the arrows), then the third spin (on the right hand) cannot satisfy its antiferromagnetic interactions with the other two spins simultaneously.

When an ordinary magnetic system is cooled sufficiently, it reaches a point where the thermal energy (which is of order  $k_B T$ ) is less than the intrinsic local magnetic exchange energy (which is proportional to the exchange constant  $J$ , the size of the magnetic moment and the number of neighboring spins). When this happens, the disordering effects of temperature succumb to the ordering effects of the magnetic interactions, resulting in what is called *magnetic order*. The spatial extent of the magnetic order, short or long range, depends on the dimensionality and geometry of the interactions, and on whether the spins are quantum or classical. Three dimensional spin systems usually exhibit long range order when  $T \leq |\Theta_{CW}|$ . Here the “Curie-Weiss” temperature,  $\Theta_{CW} = \frac{JzS(S+1)}{3k_B}$  where  $z$  is the number of neighboring spins and  $k_B$  is the Boltzmann constant. Details about the geometry and periodicity of the magnetic order will depend on the type and strength of the magnetic interactions between the moments, and are precisely the information that neutron *elastic* scattering provides.

When the magnetic lattice is geometrically frustrated, the effects of frustration can suppress the ordering transition temperature and lead to complex low-temperature phases that are qualitatively different from those present in conventional magnetic systems. To assist the experimentalist in framing the relevant questions to ask when studying such novel systems, and thus to help choose the right neutron scattering experiments to determine the answers, it is imperative that alternative sources of data, e. g. derived from literature searches, be obtained whenever available. This is discussed in the following section.

## A. Initial Experimental Planning

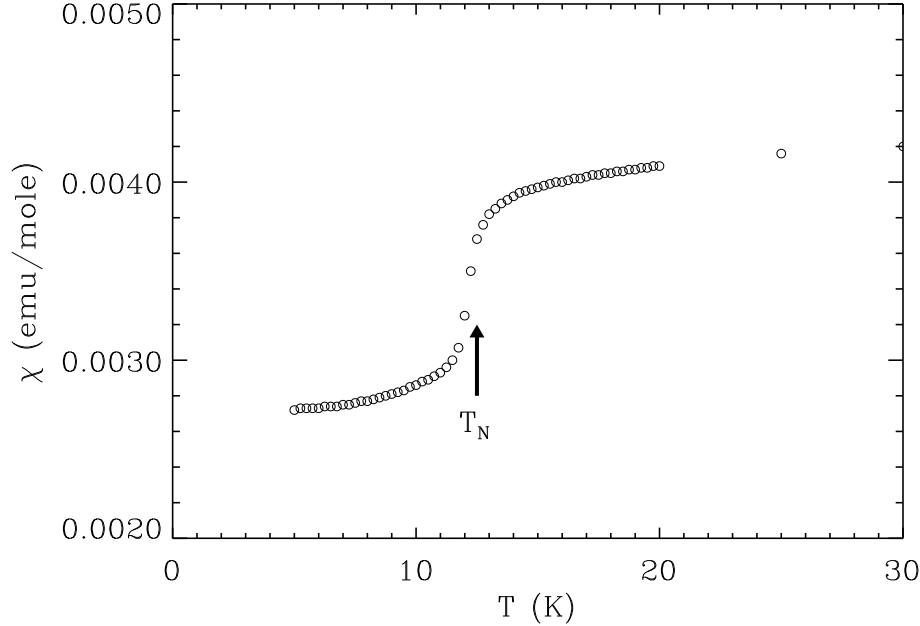


Fig. 5. Bulk susceptibility data from  $\text{ZnCr}_2\text{O}_4$ .

When planning neutron scattering experiments on a sample, measurements of bulk properties such as the magnetic susceptibility, heat capacity and resistivity, can serve as an invaluable guide. All NCNR facility users should avail themselves of any existing data, be it their own, or published elsewhere, that could help them make more efficient use of their beam time which costs NIST an average of \$4,000 per day per instrument to provide. Fig. 5 shows bulk magnetic susceptibility data taken on a powder sample of  $\text{ZnCr}_2\text{O}_4$  in which a sudden drop in  $\chi$  takes place at the transition temperature  $T_N = 12.5$  K, suggesting the occurrence of a magnetic phase transition in which the low-temperature phase exhibits an antiferromagnetic-like ordering (thereby resulting in a smaller total moment). These data show that the relevant temperature scale is 12.5 K, and that a reduction of the magnetism has occurred for reasons unknown. The relevant questions then become:

**Question:**

- (1) How does  $\text{ZnCr}_2\text{O}_4$  order magnetically below 12.5 K?
- (2) How do the correlations between spins change through the apparent phase transition at 12.5 K?

As you will see from the data you obtain, neutron scattering is an irreplaceable tool for studying the geometry and energetics of the correlations between spins in magnetic systems.

### B. Experimental Set-Up

A 25 gram powder sample of  $\text{ZnCr}_2\text{O}_4$  has been sealed inside an aluminum container. Aluminum is among the most commonly used materials for sample containers because it is relatively transparent to neutrons. We are using a powder sample in this experiment because single crystals of  $\text{ZnCr}_2\text{O}_4$ , sufficient in size for neutron inelastic measurements, are not currently available. The aluminum container has been mounted inside a liquid-helium-filled cryostat which has been cooled down to 1.5 K, and placed on top of the SPINS goniometer (or sample) table.

The incident neutron energy on SPINS can be varied from  $2.4 \leq E_i \leq 14$  meV. A 6-inch, liquid-nitrogen cooled, polycrystalline BeO filter, which transmits only neutrons having energies below the Bragg cutoff energy of 3.7 meV, Bragg scatters all other neutrons out of the transmitted beam. It has been placed after the sample to eliminate higher-order ( $n > 1$ ) monochromatic components passed by the monochromator. The energy of the center analyzer blade has been set to 3.15 meV, and the energy range that the detection system (analyzer+PSD) detects set to  $2.6 \leq E_f \leq 3.7$  meV.

**Question:** Why is the SPINS BeO filter cooled?

### C. The Spin-Spin Correlation Function $\langle S_{\mathbf{R}}(t) \cdot S_{\mathbf{R}'}(0) \rangle$

The intensity of neutrons scattered from the magnetic moments in a solid is proportional to the spin-spin correlation function

$$\frac{d^2\sigma}{d\Omega dE_f} = r_0^2 \frac{k_f}{k_i} \left| \frac{g}{2} F(Q) \right|^2 \sum_{\alpha\beta} (\delta_{\alpha\beta} - \hat{Q}_\alpha \hat{Q}_\beta) \frac{1}{2\pi\hbar} \int dt e^{i\omega t} \frac{1}{N} \sum_{\mathbf{R}\mathbf{R}'} \langle S_{\mathbf{R}}^\alpha(t) S_{\mathbf{R}'}^\beta(0) \rangle e^{-i\vec{Q}\cdot(\mathbf{R}-\mathbf{R}')} \quad (15)$$

where  $r_0 = -0.54 \cdot 10^{-12}$  cm,  $g$  is the gyromagnetic ratio,  $F(Q)$  is the magnetic form-factor and  $N$  is the number of unit cells in the solid.

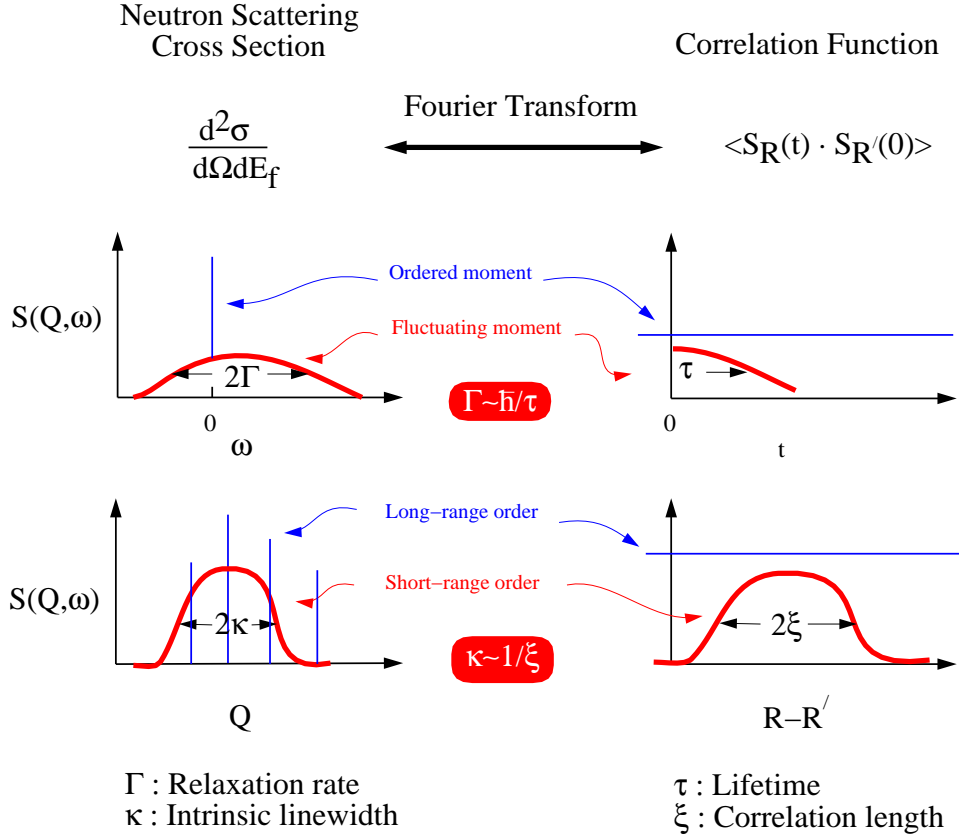


Fig. 6. The relationship between the neutron scattering cross section and the spin-spin correlation function. The relaxation rate  $\Gamma$  is HWHM in energy of  $S(Q, \omega)$ , and is inversely proportional to the lifetime of the excitation  $\tau$ . The linewidth  $\kappa$  is the HWHM in momentum transfer of  $S(Q, \omega)$ , and is inversely proportional to the correlation length  $\xi$ .

While this equation appears formidable, the following figure can help shed substantial light on the relationship between the measured magnetic neutron scattering cross section  $d^2\sigma/d\Omega dE_f$  and the time-dependent spin-spin correlation function  $\langle S_R(t) \cdot S_R(0) \rangle$ . Basically the partial differential scattering cross section  $d^2\sigma/d\Omega dE_f$  is the Fourier transform in space and time of the spin-spin correlation function. Thus, neutron elastic scattering probes static ordered moments, whereas neutron inelastic scattering probes fluctuating (dynamic) moments. The spatial dependence of the spin correlations can be determined from the  $Q$ -dependence of  $S(\vec{Q}, \omega)$ . For example, if  $S(\vec{Q}, \omega)$  is  $Q$ -resolution limited, then this would indicate that the spatial correlations are of long-range. However, if  $S(\vec{Q}, \omega)$  is broader than the instrumental  $Q$ -resolution, then the correlations are short-ranged.

Although mapping out the scattering cross section in  $(Q, \hbar\omega)$ -space is necessary, two quick scans would be a good start for this investigation: (1) Elastic measurements scanning  $Q$  both above and below  $T_N$ , for example at 1.5K and 15K. These data could be used to see if the spins in the system order below  $T_N$ , and if so, what kind of order takes place. (2) Inelastic measurements at a fixed  $Q$ , for example at  $1.5 \text{ \AA}^{-1}$ , as a function of  $\hbar\omega$  at the same two temperatures to see how the energy spectrum changes.

### III. DATA AND ANALYSIS

Fig. 7 shows the data that we should obtain. The elastic scattering intensity  $S(Q, \hbar\omega = 0)$  at 15 K exhibits a peak at  $1.31 \text{ \AA}^{-1}$  which corresponds to the nuclear (111) Bragg reflection. At 1.7 K, additional sharp peaks appear which are due to the ordering of the  $\text{Cr}^{3+}$  magnetic moments. The nuclear (111) Bragg peak is necessarily  $Q$ -resolution limited because  $\text{ZnCr}_2\text{O}_4$  is a crystal with long-range nuclear order.

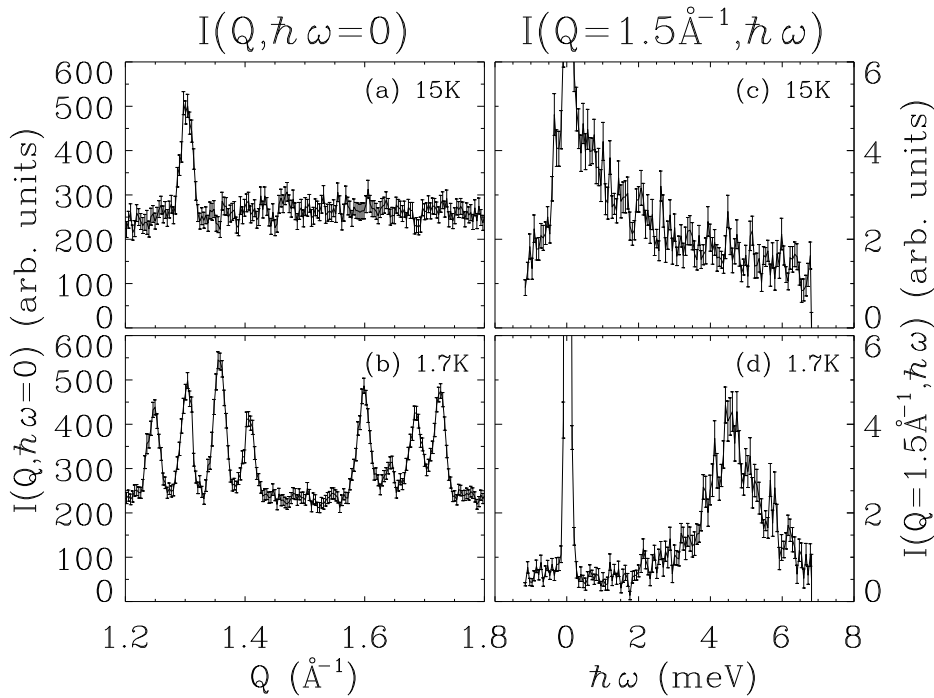


Fig. 7. (a), (b) Neutron elastic scattering data taken at 15 K and 1.7 K. (c), (d) Neutron inelastic scattering data taken at  $Q=1.5 \text{ \AA}^{-1}$  at 15 K and 1.7 K.

**Question:**

- (1) Estimate the instrumental  $Q$ -resolution.
- (2) Are the *static* spin correlations below  $T_N$  long ranged or short ranged ?

From the relative intensities of the magnetic Bragg reflections, we can determine the

spin structure of the ordered state. However the details of such an analysis are beyond this session. In fact, the true spin structure has yet to be solved.

Now we turn our attention to the magnetic excitations shown in Fig. 7 (c) and (d). At 15 K, there is strong scattering at low energies. We can roughly estimate the relaxation rate  $\Gamma$ , which is the Half-Width-at-Half-Maximum (HWHM) of  $S(\omega)$ :  $\Gamma \sim 1.3$  meV. This means that the dynamic correlations at this temperature have a lifetime of about  $\hbar/\Gamma \sim 0.5 \cdot 10^{-12}$  s. At 1.5 K, in the ordered state, the energy spectrum becomes drastically different. Most of spectral weight at low energies at  $T > T_N$  has moved into a prominent peak at  $\hbar\omega = 4.5$  meV. This peak is unusually sharp for an ordinary ordered state and is usually due to a transition between two energy levels.

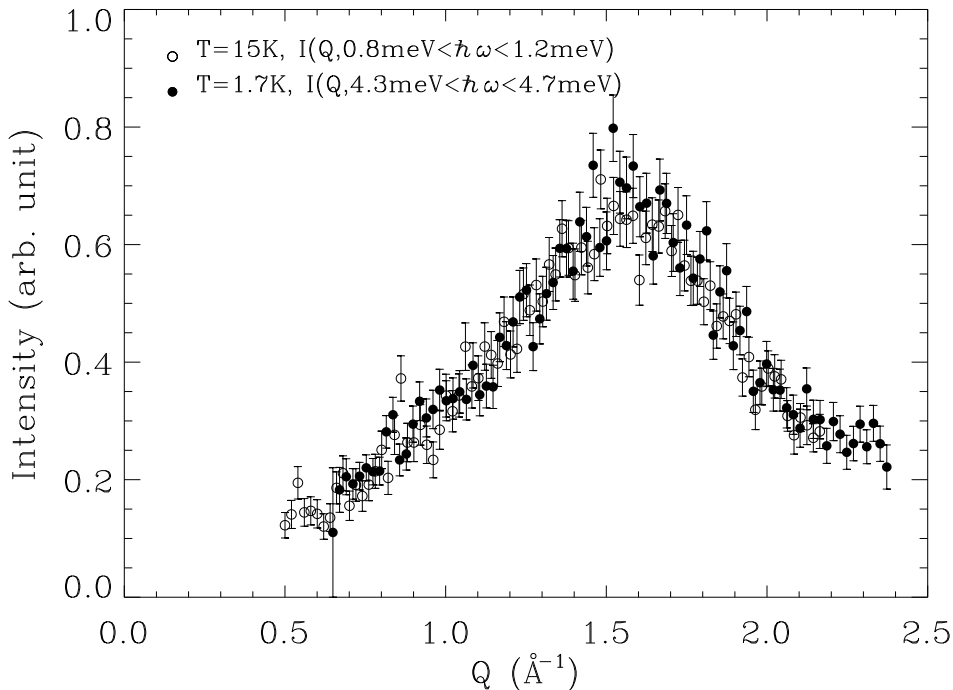


Fig. 8.  $Q$ -dependence of the inelastic scattering cross section measured using different energy ranges at different temperatures.

The spatial dependence of the spin-spin correlation function will shed light on what is responsible for the local resonance at 4.5 meV below  $T_N$ , and the low-energy excitations



above  $T_N$ . In order to obtain such information, the following two measurements are useful: (1) At 15 K, scan  $Q$  with  $\hbar\omega = 1$  meV and (2) at 1.7 K,  $Q$ -scan with  $\hbar\omega = 4.5$  meV. The results that you should get are shown in Fig. 8.

**Question:** Are the *dynamic* spin correlations long-ranged or short-ranged above and below  $T_N$  ? Estimate the correlation length,  $\xi$ , for the dynamic spin correlations.

Your estimate for  $\xi$  should suggest that the fluctuations involve *small* antiferromagnetic clusters. The broad peak at 1.7 K also indicates that there is a local spin resonance in the magnetically long-range ordered phase. The coexistence of long-range order and the local resonance is very unusual. This indicates the presence of weakly interacting spin clusters within the ordered phase, which is a key feature of geometrically frustrated magnets. To identify definitely the origin of the local spin excitations would require neutron scattering measurements on single crystals of the material.

#### IV. CONCLUSIONS

We have found that  $\text{ZnCr}_2\text{O}_4$  undergoes a phase transition from a paramagnetic phase to a long-range, antiferromagnetically-ordered phase with an unusual local spin resonance at  $\hbar\omega = 4.5$  meV. What is the mechanism of this phase transition? One possible scenario is that there are two competing phases in this material: one a cooperative paramagnetic phase with short-range order, and the other a phase with long-range order and a local spin resonance. Above  $T_N = 12.5$  K, the cooperative paramagnetic state with its high ground state degeneracy is favored due to its higher entropy. But at lower temperatures, a small crystalline distortion induces the long-range AFM order which has a lower ground state energy than the disordered paramagnetic state does. This lower ground state energy outweighs the entropy term in the free energy at low temperatures and favors the ordered phase. The short-range-ordered low-energy fluctuations at  $T > T_N$  still survive in the ordered phase because of the geometrical frustration, but since the ground state energy has decreased, the energy of the local excitation is now enhanced in  $\text{ZnCr}_2\text{O}_4$  to 4.5 meV. The fact that  $S(Q)$  has the same  $Q$ -dependence in both the paramagnetic ( $T > T_N$ ) and ordered ( $T < T_N$ ) states supports this scenario.

## REFERENCES

- [1] J. Villain, *Z. Phys. B* **33**, 31 (1979).
- [2] S.M. Lovesey, *Theory of Thermal Neutron Scattering from Condensed Matter*, (Clarendon Press, Oxford) 1984.
- [3] R. Pynn, *Neutron Scattering - A Primer*, Los Alamos Science Summer (1990).
- [4] S.-H Lee, C. Broholm, T.H. Kim, W. Ratcliff II, and S-W. Cheong, *Phys. Rev. Lett.* **84**, 3718 (2000).
- [5] S.-H Lee, C. Broholm, G. Aeppli, T.G. Perring, B. Hesse, and A. Taylor, *Phys. Rev. Lett.* **76**, 4424 (1996).